Environmental Health Engineering and Management Journal 2022, 9(3), 261-270
http://ehemj.com
doi 10.34172/EHEM.2022.27

Environmental Health Engineering and Management Journal

Original Article

Environmental Health Engineering and Management

Open Access Publish Free

Evaluation of adsorption efficiency of activated carbon functionalized with methyl diethanolamine in carbon dioxide gas

Ali Haghmoradkhani[1], Alireza Pardakhti[2*], Mohammad Ali Zahed[3]

[1]School of Environment, Kish International Campus, University of Tehran, Tehran, Iran
[2]School of Environment, College of Engineering, University of Tehran, Tehran, Iran
[3]Faculty of Biological Sciences, Kharazmi University, Tehran, Iran

Abstract

Background: Adsorption is a process in which some of the components in the fluid phase, are selectively transferred to the surface of the porous solid particles in the filled bed, which is called the adsorbent. The aim of this study was to examine the adsorption effectiveness of CO_2 by activated carbon functionalized with methyl diethanolamine (MDEA), as well as the effects of adsorption temperature, the total pressure of adsorption, and mass of adsorbent.

Methods: Activated carbon was first produced using the desired biomasses and suitable activated carbon was chosen. The activated carbon was then functionalized with MDEA amination method. The crystal structure of adsorbents was studied using X-ray diffraction (XRD) methods. In addition, the porosity, specific surface area and structure of prepared activated carbon were measured using BET techniques. Finally, the morphology and strength of the functional groups were measured using Field emission scanning electron microscopy (FESEM) and Fourier-transform infrared spectroscopy (FTIR) analyses.

Results: The findings of the FESEM and BET analyses for functionalized activated carbon revealed that the specific surface area of the adsorbent increased throughout the chemical and physical modification process, resulting in a BET amount of 725/84 m^2/g. The results showed that the selectivity of the functionalized activated carbon is greater than that of the non-functionalized adsorbent.

Conclusion: The adsorption capacity of functionalized activated carbon was 3.98 mmol CO_2 g^{-1} sorbent, compared to 2.587 mmol CO_2 g^{-1} sorbent in the non-functionalized carbon, indicating a 35% improvement in the efficiency of the functionalized sample. According to the findings of the desorption experiments, functionalized carbon shows a 25% decrease in CO_2 adsorption efficiency after 20 desorption steps.

Keywords: Activated carbon, Methyldiethanolamine, Amination, Carbon dioxide

Citation: Haghmoradkhani A, Pardakhti A, Zahed MA. Evaluation of adsorption efficiency of activated carbon functionalized with methyl diethanolamine in carbon dioxide gas. Environmental Health Engineering and Management Journal 2022; 9(3): 261-270. doi: 10.34172/EHEM.2022.27.

Article History:
Received: 8 October 2021
Accepted: 15 November 2021
ePublished: 14 August 2022

***Correspondence to:**
Alireza Pardakhti
Email: alirezap@ut.ac.ir

Introduction

Carbon dioxide (CO_2) from fossil fuels has the greatest impact on greenhouse gas emissions and global warming (1). Iran emits about 500 million tons of CO_2 per year, and is ranked ninth in the world (2). The use of CO_2 capture and storage methods for this purpose consists of three steps: Separation of CO_2 with acceptable purity (around 90%), compaction, transfer of dense CO_2 to underground reservoirs, and finally, storage of dense CO_2 underground reservoirs. Because the first stage accounts for 70%-90% of operational expenses, the CO_2 separation stage focuses on most research (3,4). According to the American Physical Society (APS), CO_2 costs $600 per ton on a large scale; therefore, a high-efficiency and cost-effective process is critical to capture carbon dioxide from flue gas (5).

Depending on the type of feed from which CO_2 is released, there are two ways to collect CO_2 from the gas stream:

- Method 1: Separation of CO_2 from the gas stream before combustion.
- Method 2: Separation of CO_2 from the gas stream after combustion.

Easier separation of CO_2/H_2 from CO_2/N_2 is one of the advantages of the first method and disadvantages of the second method (6). CO_2 capture technologies can be categorized into three groups: Precombustion CO_2 capture, post-combustion CO_2 capture, and oxy-fuel combustion (7). Carbon materials such as activated carbon, molecular carbon particles, carbon nanotubes and graphene are the most important physical adsorbents (8). Carbon nanotubes are used in most aqueous solvents according to their physical, chemical, and electrical properties (9). The structural properties of carbon can be modified by

activation (10). The carbonization temperature will vary depending on the type of raw material, but is usually between 400-500°C (11). Inexpensive carbon sources are readily available and can reduce the cost of preparation on an industrial production scale (12). Carbon is physically activated by water vapor and chemically activated by phosphoric acid (13). Improving soil quality (14), eliminating emerging contaminants in soil and water (15), and reducing greenhouse gas emissions and energy production are among different applications of carbon (16). The adsorption properties of activated carbon vary according to the type of raw materials and production conditions (17,18).

Pertiwiningrum et al studied the application of activated carbon derived from biogas sludge and the optimal conditions for biogas treatment. Biochar-based biogas sludge was tested in five treatments, the absorbent columns contained 100% zeolite, 50% zeolite and biochar, 25% zeolite, and 75% biochar, and finally, 100% biochar. They found that all five treatments decreased CO_2 (impurity gas in biogas) and 100% of the volume biochar treatment had the highest efficiency in reducing CO_2 (4).

In a research, the simulation of carbon dioxide (CO_2)-methane (CH_4), gas adsorption, and the selectivity on zeolite 4A using Aspen Adsorption were investigated. In the binary system, some effective factors such as temperature, pressure, and different combinations of CO_2 were tested. The results showed that the maximum efficiency for adsorption of CO_2 and CH_4 are obtained at 273°K and 10 bar in the Langmuir isotherm model with 5.86 and 2.88 mmol/g, respectively (19, 20).

Carbon molecular sieves and zeolite 5A performance in a 4-bed vacuum pressure process with swing adsorption was compared. The separation of CO_2 from a CH_4/CO_2 mixture gas, such as coal bed methane or landfill gas was the goal of this process. The findings indicated that under low-pressure conditions and vacuum pressure of 1000 Pa, zeolite 5A is more efficient and powerful than carbon molecular sieve (21).

A study was conducted on the metallized biochar development as a low-cost bio-sorbent to obtain high adsorption capacity for eliminating low-temperature CO_2. For making biochar from rambutan peel (RP) at various temperatures, single-step pyrolysis process was done. The biochar product placed under wet impregnation conditions with several magnesium salts, which subsequently, underwent heat-treated with N_2. The efficiency of CO_2 capture was improved by impregnating magnesium into the biochar structure, and the magnesium nitrate, magnesium sulphate, magnesium chloride, and magnesium acetate were effective, respectively. The results showed that CO_2 absorption capacity of metallized biochar (76.80 mg g^{-1}) was higher than pristine biochar (68.74 mg g^{-1}) (22).

Esfandian and Garshasbi reported Kaolin, Bentonite, and Feldspar as low-cost sources of Si and Al to synthesize the molecular sieve 13X. The adsorption capacities (pressure >20 bar) of 13X (kaolin), 13X (bentonite), and 13X (feldspar) were 3.6, 2.4, and 1.95 mmol/g, respectively. The adsorption data were fitted to some isotherms including Langmuir, Freundlich, Sips, BET, and Toth. It was found that the Sips model showed better fitting in comparison to other models (23).

Ghalandari et al investigated two types of activated carbon adsorbents and the equilibrium adsorption isotherms of N_2, CH_4, and CO_2. The findings showed that the Sips isotherm model is an appropriate model for forecasting the behavior of gas adsorption (24).

Carbon dioxide separation is now carried out on an industrial scale using the adsorption technique and amine solutions. The drawbacks of this technique include severe equipment corrosion, energy-consuming amine solution recovery, and environmental contamination during solvent recovery. The adsorption technique offers an alternative to conventional separation procedures on a smaller scale due to its low energy consumption. The selection of a suitable adsorbent may play a major role in reducing the cost of CO_2 separation and storage (25).

In this study, the absorption performance of activated carbon functionalized by methyl diethanolamine (MDEA) for post-combustion CO_2 capture was examined as an inexpensive approach for flue gas separation. Activated carbons show an excellent performance in CO_2 capture due to its beneficial characteristics, such as a high activity level and high chemical active sites. To the best of our knowledge, this is the first study that used activated carbon to absorb CO_2 pollutants. It is worth noting that flue gas in the form of standard reference capsules was used.

Materials and Methods

Preparation of activated charcoal

In this study, hard walnut shell and pistachio shell were used to prepare activated carbon.

Preparation method

The selection of biomass and its processing as a raw material is the first stage in the pyrolysis process and carbon preparation. The cellulose and lignin contents of the biomass, the moisture content, and the size of pieces (fragments) are the most significant parameters that influence the preparation and performance of carbon. Before processing raw material, it is desirable to remove impurities such as dirt, gravel, and other wastes. In this study, hard walnut shell and rice hulls were used to prepare activated carbon.

Carbon preparation by neutral gas

In this technique, vapors of volatile material are not directly linked to the furnace outlet and instead enter the electric furnace area. The furnace area is connected to neutral gas, which sends the vapors to the furnace outlet.

The essential feature of this technology is that holes are punched in the pyrolysis reactor wall to enable volatile vapors from within the reactor to escape. The reactor cap may be adjusted or removed entirely to transport vapors from the reactor to the furnace area, depending on the kind of vessel and the weight of the raw material sample. Vapors may escape from the gap between the reactor's door and vessel if the reactor door diameter is greater than the reactor vessel diameter.

Preparation of materials and equipment

According to scientific papers and past research, as well as preliminary estimates, the necessary chemicals were prepared without contaminants in the appropriate amounts from renowned brands such as Sigma-Aldrich and Merck. An electrochemical sensor and an infrared bench were used to measure the quantity of CO_2 in gas meters. In addition, X-ray diffraction (XRD), Field emission scanning electron microscopy (FESEM) , BET, and Fourier-transform infrared spectroscopy (FTIR) were used to examine the morphology and crystal structure of the prepared adsorbents.

In order to synthesize activated carbon, hard walnut shell and pistachio shell were prepared in an appropriate volume and according to standard laboratory methods, drying and preparation of activated carbon with appropriate porosity were done. After synthesis, carbon was modified to get the required characteristics. Functionalization is a chemical procedure that involves adding functional groups to the carbon in order to improve the interaction between the matrix and the amplifier. Carbon can absorb a wide range of organic and inorganic chemicals due to this process. Functionalization may be accomplished in a variety of ways, including oxidation, fluoridation, esterification, plasma, and amination. In this study, functionalization was performed using an ultrasonic device at a temperature of 30°C for 8 hours of exposure to activated carbon with the amine group.

The impact of factors such as adsorption temperature, the total pressure of adsorption and mass of adsorbent on thermodynamic parameters, equilibrium isotherms, and adsorption process kinetics was investigated.

The recovery and reusability tests of the adsorbents were also performed. Based on the specified parameters and tests conducted, as well as the results of the completed analyses, the findings were then evaluated and summarized in order to obtain realistic outcomes. It is worth noting that independent variables were pressure, adsorbent dosage, and gas temperature. Moreover, dependent variables were gas adsorption capacity and its residue. According to the dimensions of the electric muffle furnace, a sample weight of a maximum of 100 g of dried raw material based on the required contents in each pyrolysis reactor is adequate.

A certain volume of adsorbent substrate was subjected to the specified concentration of CO_2 gas, and then, its concentration was read directly before entering the substrate and after leaving the substrate. Afterwards, variable adsorption parameters such as temperature, pressure, and mass of adsorbent in different states were measured. Before starting the study, preliminary operation tests including calibration of all devices including pressure gauge, flowmeter, air compressor performance test, hydrotest of equipment and fittings, charging of the adsorbent bed from the desired carbon, checking gas reference capsules, air compressor test and pressure adjustment and gas analyzers test. At first, air passed through the system for a relatively long time until the temperature and humidity on both sides of the test column reached equilibrium.

The crystal structure of the prepared adsorbents was studied using XRD methods, while specific area and porosity were measured using BET. The morphology of the constructed adsorbents and the strength of functional groups were determined using FESEM and FTIR analyses, respectively. Then, the effectiveness of the prepared adsorbents for CO_2 capture was assessed by establishing test conditions and conducting the test. Schematic diagram of surface adsorption system is presented in Figure 1.

Results

BET results

Two samples of carbon made from hard shells of walnuts and pistachio shell were transported to the laboratory to determine the sample that had the best particle surface area for the adsorption process in the BET test. Finally, sample B was chosen as the final carbon, which comprised hard shells of walnuts with a BET of 725.84 m^2/g. The amination process was then performed on the carbon with a 20% MDEA solution, a tertiary amine with a high capacity for gas absorption. A BET test was conducted on the animated carbon to evaluate changes in cavity volume, the findings of which are reported in the tables. The BET test findings for carbons are presented in Table 1.

The BET of carbon (hard shells of walnuts)

The N_2 gas adsorption isotherm spectrum of the walnut carbon sample is aligned with type I six IUPAC (International Union of Pure and Applied Chemistry) curves and has a specific pore area of 719.77 m^2/g, which is greater than the other two carbons. The desorption and hysteresis curves are aligned with type H_4 IUPAC curves. The cavities seem to be thin, layered, and saucer-shaped. The cavity is linked from the exterior side. The cavities frequency with a radius of 1° and in micro size may be calculated using the BJH curve and the value of r_{peak} = 1.21 mm. According to the TPLOT curve, the micro surface is computed as follows:

$$a\,micro = a_1 - a_2 \quad (1)$$

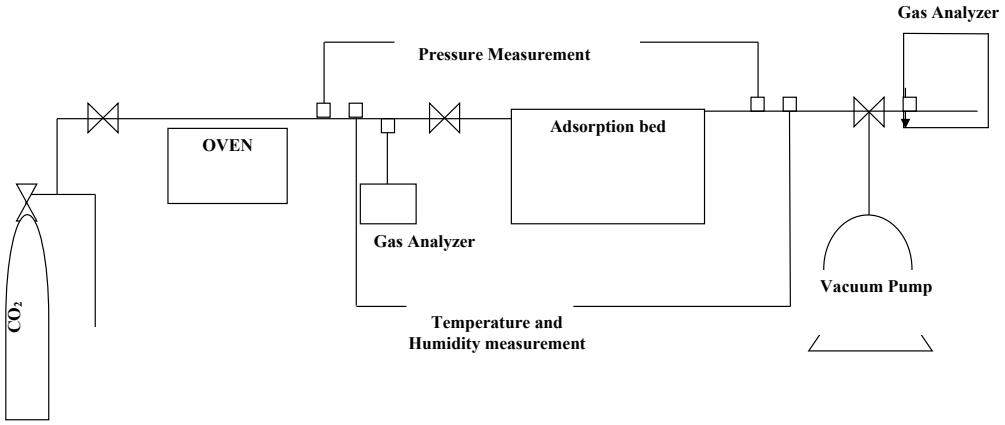

Figure 1. Schematic diagram of surface adsorption system.

Table 1. Results of the specific surface area of cavities in four carbon samples

NO.	Parameter	Sample A	Sample B	Sample C
1	Volume (cm^3/g)	0.1243	0.4498	0.2399
2	Diameter (mm)	2.4145	2.4986	1.8999
3	BET (m^2/g)	185.22	719.77	503.43

Sample A: Pistachio shell, Sample B: Hard shells of walnuts, Sample C: Hard shells of walnuts functionalized by MDEA.

$$a\,micro = 758.65 - 24.752 = 733.897\,m^2 / g \quad (2)$$

Adsorption isotherm spectrum of the walnut carbon N_2 gas adsorption isotherm, desorption and hysteresis curves, BJH diagram to investigate the radius of frequency of cavities and micro surface in the TPLOT curve are presented in Figure 2.

The BET of animated walnut carbon

The N_2 gas adsorption isotherm spectrum of the animated walnut carbon sample is aligned with type I IUPAC curves and has a specific pore area of 503.43 m^2/g. Adsorption isotherm spectrum of the animated walnut carbon, N_2 gas adsorption isotherm, desorption and hysteresis curves, BJH diagram to investigate the radius of frequency of cavities and micro surface in the TPLOT curve are presented in Figure 3.

The desorption and hysteresis curves are aligned with type H4 IUPAC curves. The cavities seem to be thin, layered, and saucer-shaped. The cavity is linked from the exterior side. The cavities frequency with a radius of 1° and in micro size may be calculated using the BJH curve and the value of r_{peak} = 1.21 mm. The micro surface is computed as follows when looking at the TPLOT curve:

$$a\,micro = a_1 - a_2 \quad (3)$$

$$a\,micro = 539.97 - 3.96 = 536.01\,m^2 / g \quad (4)$$

Based on the IUPAC classification, pore measurements in terms of diameter are divided into three categories, macropores with a diameter higher than 50 nm, mesopores with a diameter between 2 to 50 nm, and micropores with a diameter lower than 2 nm (26).

Micropores with a diameter lower than 1 nm will play an important role in the adsorption of CO_2 with activated carbon (27). According to previous studies in the pressure range of 1 bar, the size of the adsorbent pores with a diameter lower than 0.8 nm has shown better performance in adsorption (28). The size of the micropores (R2 ¼ 0.9032, n ¼ 32, Figure 1b) has a greater effect on the carbon dioxide uptake than the BET surface areas (R2 ¼ 0.6475, n ¼ 16, Figure 1a). Therefore, the type of biochar pores is an important factor in CO_2 uptake (29).

FESEM of functionalized carbon and non-functionalized carbon

The surface morphology of non-aminated carbon and aminated carbon is shown in Figure 4. Comparison of curves (a) and (b) with curves (c) and (d) showed that carbon was functionalized with an amine group. In addition, the surfaces of curves (c) and (d) get rougher during the functionalization. Furthermore, a series of cavities are created on the carbon plates, which are then opened, increasing the adsorption capacity.

Adsorption results

The test equipment of aminated carbon comprises a horizontally simulated chimney column. The device was equipped with suitable sampling regions for monitoring the speed, pressure, temperature, and concentration of the input and output gas to the adsorbent. In addition, the concentration of CO_2 gas was supplied by calibration-certified reference capsules and placed in the flow path. After the calibration procedure, instruments were placed in the appropriate places to monitor the speed, temperature, humidity, and concentration of gas metering.

A specific volume of the adsorbent substrate was exposed to a specific concentration of CO_2 and the concentration of gas was measured both before and after entering the

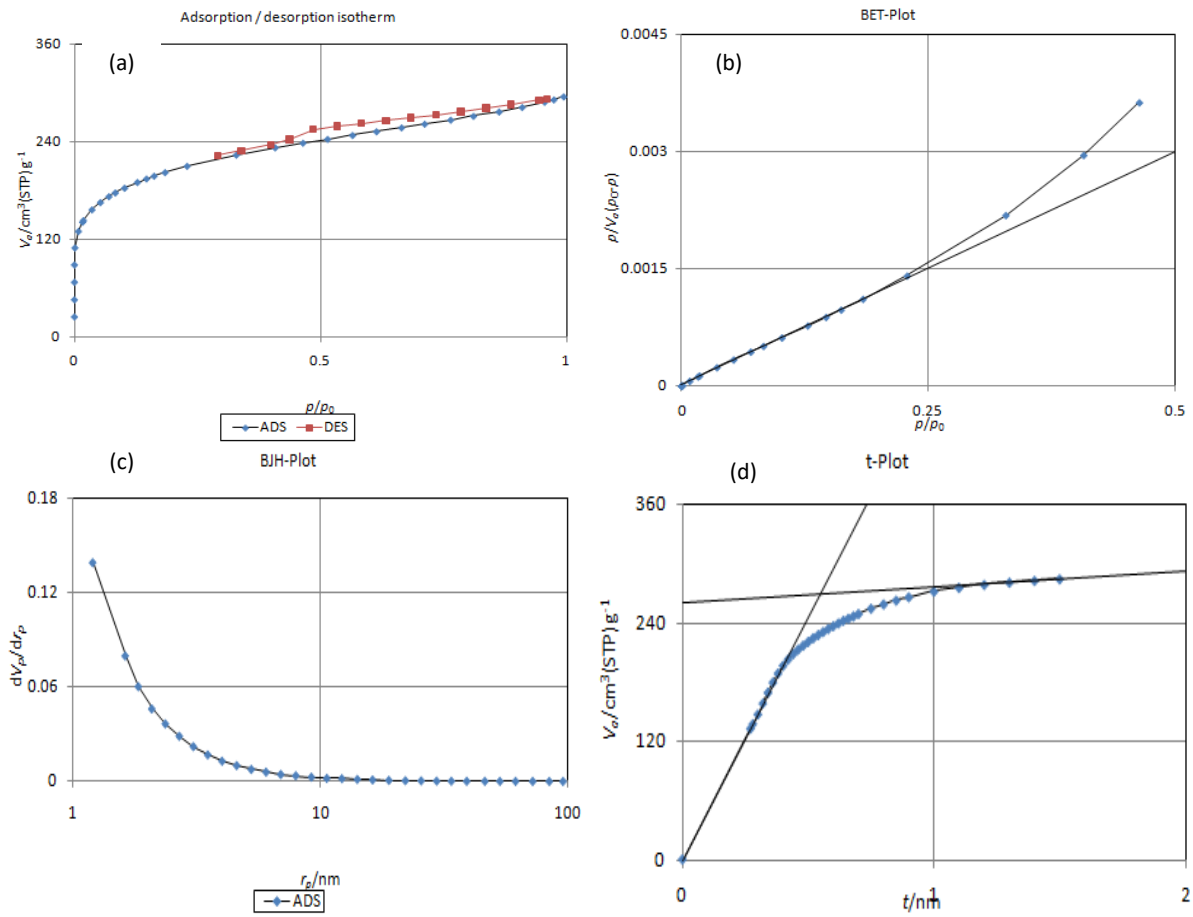

Figure 2. **(a)** Adsorption isotherm spectrum of the walnut carbon N_2 gas adsorption isotherm, **(b)** Desorption and hysteresis curves, **(c)** BJH diagram to investigate the radius of frequency of cavities, **(d)** Micro surface in the TPLOT curve.

bed. The absorption parameters, such as temperature, pressure, and adsorbent volume, were investigated in various states. Before the study, all equipment including the flowmeter, pressure gauge, charging of the adsorbent bed from the selected carbon, air compressor performance test, hydro test of equipment and fittings, air compressor test, pressure control, and gas analyzers was calibrated. Air is circulated through the system for a lengthy period at first until the humidity and temperature on both sides of the experiment column achieve equilibrium.

It is important to ensure that the test system does not leak during this procedure. Ceramic wool was used to guarantee that no leaks occurred in the equipment's fitted components. Following the above-mentioned procedures, the concentration of CO_2 before entering the system and after exiting the adsorbent was measured at regular intervals (every 60 seconds) and all variable parameters were evaluated, and corresponding isotherms were produced. After 20 stages of adsorption and desorption, the optimum conditions for adsorbent efficiency were established, and the adsorbent efficiency was ultimately assessed. The adsorption and desorption paths were investigated at a temperature of 120°C and a vacuum pressure of 0.02 bar. The separation of CO_2 from the surface of the prepared adsorbent in the desorption stage was anticipated to be more challenging due to the hysteresis ring and the absorption enthalpy of CO_2 from the carbon surface. Also, it was anticipated that a bigger desorption ring would be produced. The vacuum pump was switched on after the adsorption by applying a vacuum of 0.02 bar at a temperature of 120°C for 1 hour every 10 minutes. The adsorbent was put in the gas flow path after the desorption process to examine the adsorption effectiveness. It is worth noting that the intake flow should be regulated so that the gas leaves the adsorbent surface in less than 0.2 seconds. Mass of adsorbent, temperature, pressure, initial concentration of CO_2, concentration of CO2 after adsorbent, and concentration of CO_2 after functionalized adsorbent (ppm) are presented in Tables 2 and 3. The results of adsorption of functionalized carbon and non-functionalized carbon as well as the results of desorption of adsorbent are shown in Tables 4 and 5.

At a temperature of 30°C and a pressure of 1 bar, the optimum adsorbent conditions were 40 cm in length and 5 cm in height. The adsorption effectiveness diminishes as the temperature rises. Adsorption is enhanced by increasing the length of the adsorbent and the pressure. It should be mentioned that the adsorbent arrangement

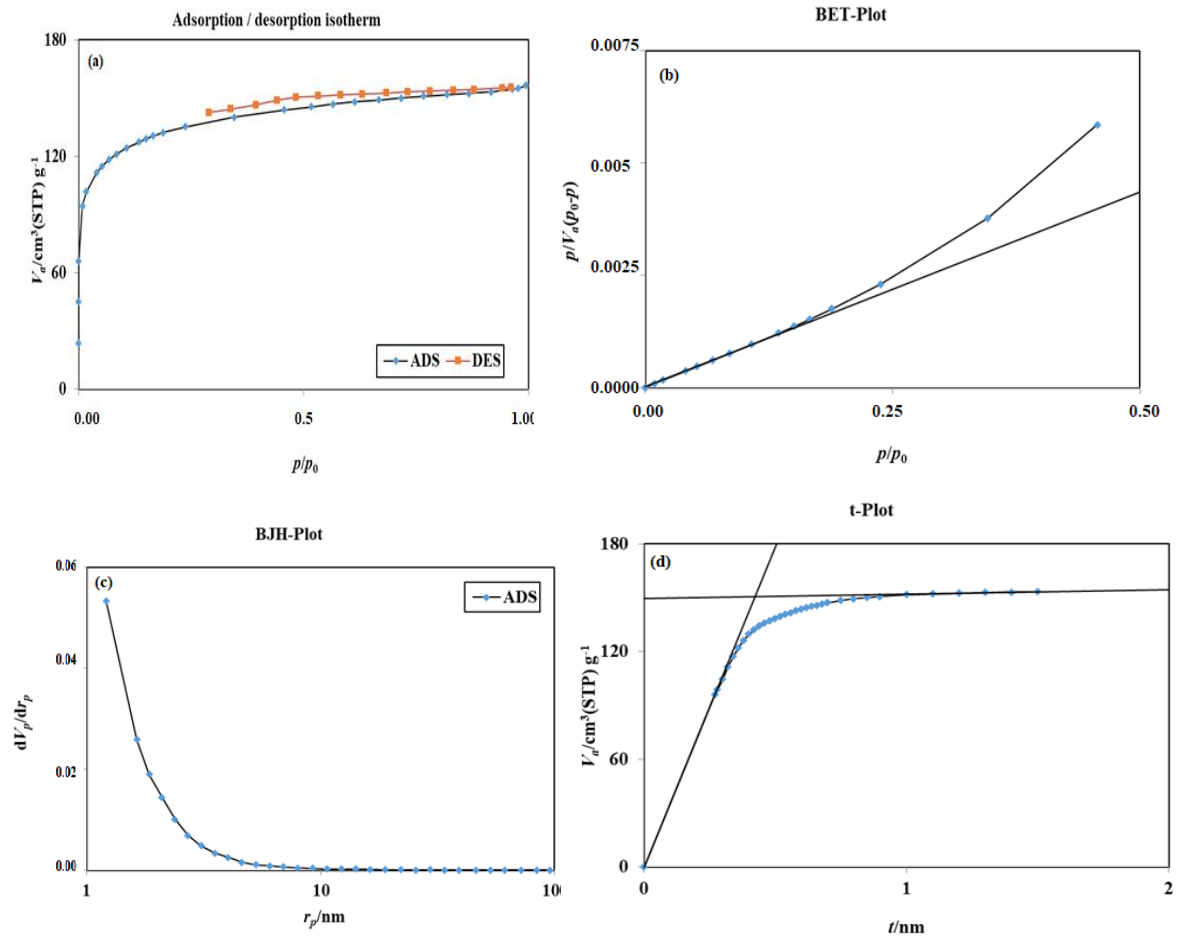

Figure 3. **(a)** Adsorption isotherm spectrum of the animated walnut carbon. N_2 gas adsorption isotherm, **(b)** Desorption and hysteresis curves, (**c)** BJH diagram to investigate the radius of frequency of cavities, (**d)** Micro surface in the TPLOT curve.

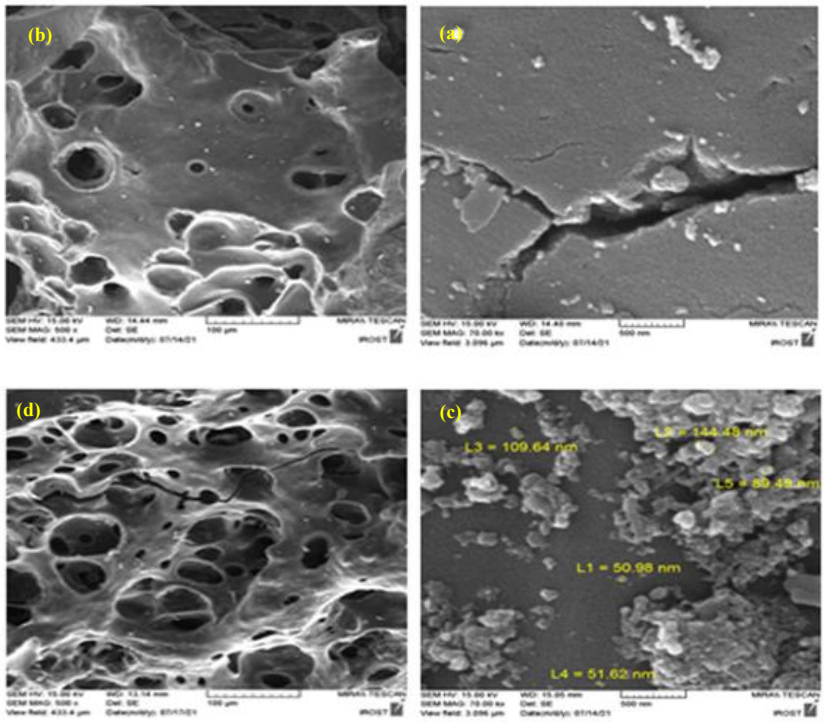

Figure 4. Surface morphology of the non-aminated carbon and the aminated carbon: (**a)** Non-functionalized carbon adsorbent at 500 nm magnification, (**b)** Non-functionalized carbon adsorbent at 100 nm magnification, (**c)** Functionalized carbon adsorbent at 500 nm magnification, (**d)** Functionalized carbon adsorbent at 100 nm magnification.

Table 2. Test results (temperature is a variable parameter)

No.	Mass of adsorbent (g)	Temperature (°C)	Pressure (bar)	Initial concentration of CO_2 (ppm)	Concentration of CO_2 after adsorbent (ppm)
1	100	30	0.2	10000	1706
2	100	50	0.2	10000	1912
3	100	90	0.2	10000	3655

Table 3. Test results (pressure is a variable parameter)

No.	Mass of adsorbent (g)	Temperature (°C)	Pressure (bar)	Initial concentration of CO_2 (ppm)	Concentration of CO_2 after functionalized adsorbent (ppm)
1	100	30	0.2	100000	1722
2	100	30	0.7	10000	1349
3	100	30	1	10000	1167

Table 4. Results of adsorption of functionalized carbon and non-functionalized carbon

No.	Mass of adsorbent (g)	Temperature (°C)	Pressure (bar)	Initial concentration of CO_2 (ppm)	Concentration of CO_2 after non-functionalized Adsorbent (ppm)
1	100	30	1	10000	1167
No.	**Mass of adsorbent (g)**	**Temperature (°C)**	**Pressure (bar)**	**Initial concentration of CO_2 (ppm)**	**Concentration of CO_2 after functionalized adsorbent (ppm)**
2	100	30	1	10000	976

Table 5. Results of desorption of adsorbent

No.	Mass of Adsorbent (g)	Temperature (°C)	Pressure (bar)	Initial concentration of CO_2 (ppm)	Concentration of CO_2 after adsorbent (ppm)	Concentration of CO_2 after 6 desorption steps after adsorbent (ppm)	Concentration of CO_2 after 10 desorption steps after adsorbent (ppm)	Concentration of CO_2 after 20 desorption steps after adsorbent (ppm)
1	100	30	1	10000	976	1000	1056	1222

along with the transmission flow path was shown to improve adsorption efficiency in different tests. During several tests, the most appropriate adsorption efficiency was found to be 8 to 1 of the length to diameter ratio of the flow path, which is equal to 100 g of adsorbent.

According to the findings of desorption experiments, functionalized carbon shows a 25% decrease in CO_2 adsorption efficiency after 20 desorption steps. In the present study, Freundlich and Langmuir isotherms were used to determine the general adsorption capacity of CO_2 by aminated and non-functionalized carbon adsorbents. The models were also examined by the adjusted R^2. According to the findings, the Freundlich isotherm is more suitable for the adsorption of CO_2 for both non-functionalized and functionalized adsorbents because the R^2 value is more acceptable, which shows how accurate the fit is. The fit of the Langmuir isotherm, on the other hand, is also satisfactory. Langmuir and Freundlich isotherms of CO_2 adsorption with non-functionalized and functionalized adsorbent are shown in Figures 5 and 6, respectively.

The results of comparison of two isotherms of Freundlich and Langmuir in the adsorption of CO_2 from the gaseous medium with aminated and non-aminated adsorbents are presented in Table 6.

Discussion

In the present study, the feasibility investigation of periodic adsorption for CO_2 capture from flue gas with functionalized carbon with Methyldiethanolamine prepared from hard shells of walnuts and pistachio shell was examined due to the increasing importance of reducing CO_2 emissions into the environment. For the first time, carbon was made from two different biomasses, and the best carbon was chosen. Then, water vapor and phosphoric acid were used to activate carbon physically and chemically. In the adsorption process, functionalization of carbon with Methyldiethanolelamine was performed. Finally, the temperature, pressure, and mass of the adsorbent were studied.

During the chemical and physical modification process, new cavities were created in the modified adsorbent structure, and the specific adsorbent surface increased, according to the findings of FESEM and BET analyses for the chosen carbon. The activated carbon sample showed a BET of 719.77 m^2/g, which has significant benefits in terms of specific adsorbent surface and pore size.

Experiments were carried out in order to examine

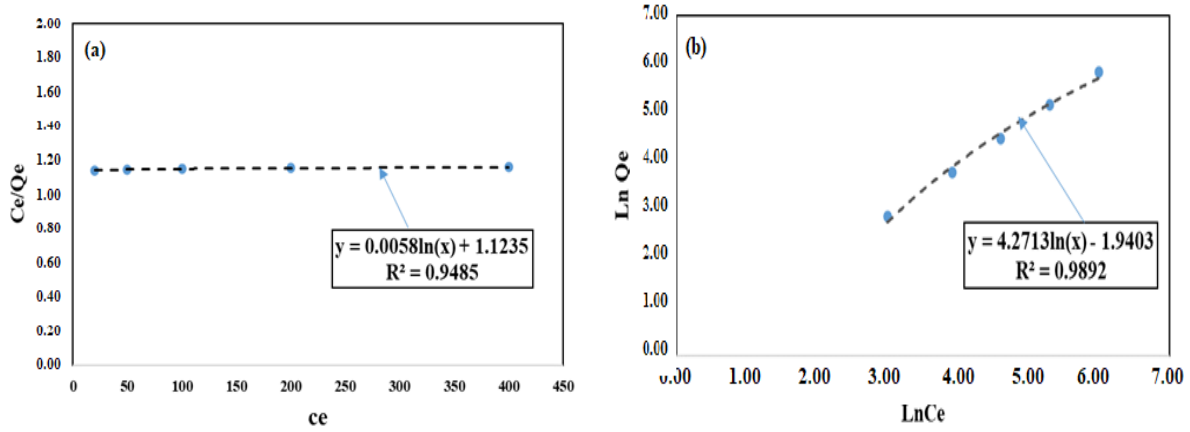

Figure 5. CO_2 adsorption isotherms with non-functionalized adsorbent: **a)** Langmuir, **b)** Freundlich.

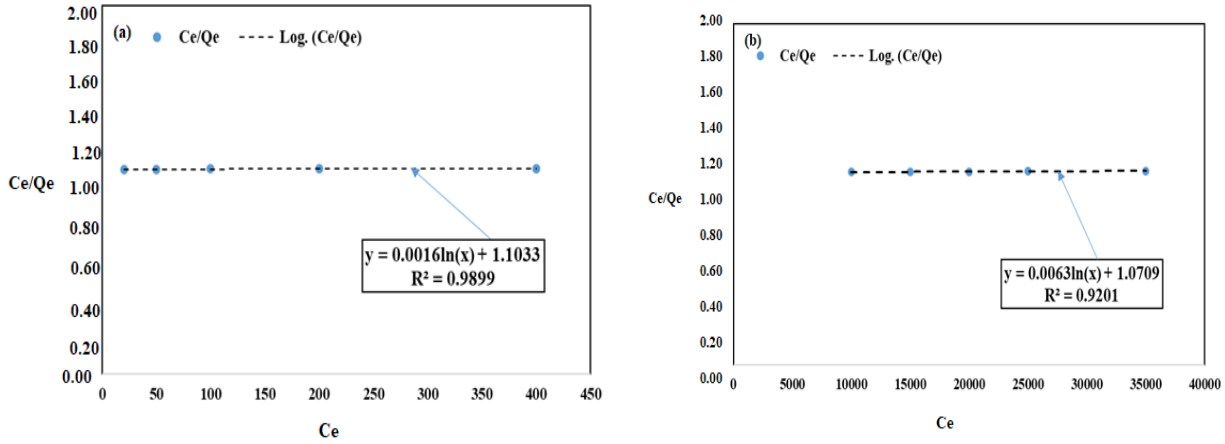

Figure 6. CO_2 adsorption isotherms with functionalized adsorbent: **a)** Langmuir, **b)** Freundlich.

Table 6. Results of CO_2 isotherms with aminated and non-aminated adsorbents

Adsorbent	Freundlich isotherm		Langmuir isotherm	
	Regression	R^2	Regression	R^2
CO_2 capture with non-functionalized adsorbent	4.2713ln(x) - 1.9403	0.9892	0.0058ln(x) + 1.1235	0.9485
CO_2 capture with functionalized adsorbent	4.2862ln(x) - 1.9277	0.989	0.0016ln(x) + 1.1033	0.9899

and assess the chemical structure of carbon in terms of the creation and development of pores as a function of activation temperature. These experiments demonstrate the chemical changes produced by the activation process with phosphoric acid. First, at temperature of 50°C, the structure of lignin undergoes substantial modifications. At 100°C, a substantial percentage of the cellulose reacts, forming esters and setens.

Phosphate esters are produced at temperatures of about 150°C. The effectiveness of activated carbon is increased by cyclic processes that start at 150°C. Low-temperature phenomena occur sooner and are linked to developing expansion pores that begin at about 250°C and reach the maximum temperature between 350°C and 450°C.

The pores volume is linked to the density of the cyclic processes up to 450°C, but beyond this temperature, there is a dimensional reduction and, eventually, a decrease in the number of pores. According to the findings of equilibrium adsorption efficiency, the functionalized adsorbent selectivity is greater than that of the non-functionalized adsorbent. This is attributed to the basic property, surface interaction with CO_2, and increased surface polarization. The adsorption capacity of functionalized activated carbon was 3.98 mmol CO_2 g^{-1} sorbent, compared to 2.587 mmol CO_2 g^{-1} sorbent in the non-functionalized carbon, indicating a 35% improvement in the functionalized sample's efficiency. Adsorption capacity of various biochars with prepared carbons from hard shells of walnuts and hard shells of pistachio are compared in Table 7 (30).

Table 7. Comparison of adsorption capacity of various biochars with prepared carbons from hard shells of walnuts and hard shells of pistachio (7,30)

Type of Biochar	The Adsorption Capacity for CO_2 Capture (mmol/g)
Roasted peanut shell waste	3.8
Peanut shell	2.1
Perilla leaves	2.312
Japanese oak	0.379
Korean oak	0.597
Soy residue	0.707
Hard shells of walnuts	3.98

In a study by Chatterjee et al, an ultrasonic activated biochar adsorbent with a pine wood source, functionalized with the amine group (tetraethylene pentaamine), was used to absorb carbon dioxide. The results showed that the porosity and permeability of biochar increased and the absorption of biochar increased more than 9 times more efficient than the untreated biochar (31).

According to the CO_2 desorption findings, the hysteresis ring is created in the desorption of two samples. Because functional groups are present on the adsorbent surface, this ring for the modified adsorbent shows a higher dimension, raising the surface polarity, ultimately, leading to more significant contact between gases and the adsorbent surface. The adsorption effectiveness of functionalized carbon for CO_2 gas capture dropped by 25% after 20 desorption stages and it was found that the CO_2 adsorption capacity of nitrogen-functionalized sawmill-residue-based biochar decreased by 4-8% after 5 cycles and by 20% after 10 cycles (7).

Conclusion

The results of adsorption investigations for functionalized carbon were obtained based on the following parameters: temperatures of 30, 50, and 90°C, adsorbent bed lengths of 30 and 40 cm, adsorbent bed widths of 5 and 15 cm, and a pressure range of 0.1-1 bar. The adsorbent bed with the greatest adsorption effectiveness corresponded to a temperature of 30°C, a pressure of 1 bar, 40 cm length, and 5 cm width. The adsorption capacity is directly proportional to the adsorbent bed length and pressure, and inversely, proportional to the adsorbent bed diameter and the temperature. Therefore, as the adsorbent bed length and pressure rise, the adsorption effectiveness increases. In addition, as the adsorbent bed diameter and temperature increase, the adsorption effectiveness decreases. According to the results, greater absorption capacity is possible when high pressures and low temperatures are approached. According to the activated carbon desorption efficiency in 20 stages, a decrease of approximately 25% in absorption efficiency, plentiful supplies of hard shells of walnuts, and the low cost of carbon preparation, carbon may be used as a high-performance adsorbent for industrial applications.

Acknowledgements

Special thanks are extended to School of Environment, College of Engineering, University of Tehran for efficient help in providing the database of this study.

Ethical issues

Not applicable.

Competing interests

The authors declare that they have no known competing financial interests or personal relationships that could have appeared to influence the work reported in this paper.

Authors' contributions

AH contributed to conception or design of the work, data collection, analysis and interpretation, drafting the article, and final approval of the manuscript. AP contributed to conception or design of the work, critical revision of the article, and final approval of the manuscript. And MAZ contributed to data collection and final approval of the manuscript.

References

1. Borhani F, Shafiepour Motlagh M, Stohl A, Rashidi Y, Ehsani AH. Changes in short-lived climate pollutants during the COVID-19 pandemic in Tehran, Iran. Environ Monit Assess. 2021;193(6):331. doi: 10.1007/s10661-021-09096-w.
2. Poursif T, Sadeghian S, Ahmadian N, Jabari T. The effect of carbon dioxide gas on humans and climate change. The 5th international congress of agricultural development and environment with emphasis on the development program of nations; Tehran: 2021.Available from: https://civilica.com/doc/1235185.
3. Nie L, Mu Y, Jin J, Chen J, Mi J. Recent developments and consideration issues in solid adsorbents for CO2 capture from flue gas. Chin J Chem Eng. 2018;26(11):2303-17. doi: 10.1016/j.cjche.2018.07.012.
4. Pertiwiningrum A, Pambudi WL, Mira L, Fitriyanto NA, Wuri MA, Harto AW. The utilization of biogas sludge biochar to lead zero waste system in biogas implementation: the effect of volume on carbon dioxide and methane content. Int J GEOMATE. 2021;20(79):119-24. doi: 10.21660/2021.79.gx388.
5. Zhang G, Zhao P, Hao L, Xu Y, Cheng H. A novel amine double functionalized adsorbent for carbon dioxide capture using original mesoporous silica molecular sieves as support. Sep Purif Technol. 2019;209:516-27. doi: 10.1016/j.seppur.2018.07.074.
6. Ben-Mansour R, Habib MA, Bamidele OE, Basha M, Qasem NAA, Peedikakkal A, et al. Carbon capture by physical adsorption: materials, experimental investigations and numerical modeling and simulations-a review. Appl Energy. 2016;161:225-55. doi: 10.1016/j.apenergy.2015.10.011.
7. Guo T, Ma N, Pan Y, Bedane AH, Xiao H, Eić M, et al. Characteristics of CO2 adsorption on biochar derived from biomass pyrolysis in molten salt. Can J Chem Eng. 2018;96(11):2352-60. doi: 10.1002/cjce.23153.

8. Yoro KO, Singo M, Mulopo JL, Daramola MO. Modelling and experimental study of the CO2 adsorption behaviour of polyaspartamide as an adsorbent during post-combustion CO2 capture. Energy Procedia. 2017;114:1643-64. doi: 10.1016/j.egypro.2017.03.1294.
9. Boyeri Hassani AR, Mirahmadi Babahidari SA. Use of nanosorbents to absorb carbon dioxide. In: Proceeding of the 4th National Conference on Civil Engineering, Architecture and Urban Development; 2018 April 7; Babol, Iran. [Persian].
10. Ünveren EE, Monkul BÖ, Sarıoğlan Ş, Karademir N, Alper E. Solid amine sorbents for CO2 capture by chemical adsorption: a review. Petroleum. 2017;3(1):37-50. doi: 10.1016/j.petlm.2016.11.001.
11. Gupta VK, Agarwal S, Saleh TA. Chromium removal by combining the magnetic properties of iron oxide with adsorption properties of carbon nanotubes. Water Res. 2011;45(6):2207-12. doi: 10.1016/j.watres.2011.01.012.
12. Chen Z, Deng S, Wei H, Wang B, Huang J, Yu G. Activated carbons and amine-modified materials for carbon dioxide capture-a review. Front Environ Sci Eng. 2013;7(3):326-40. doi: 10.1007/s11783-013-0510-7.
13. Jiao J, Cao J, Xia Y, Zhao L. Improvement of adsorbent materials for CO2 capture by amine functionalized mesoporous silica with worm-hole framework structure. Chem Eng J. 2016;306:9-16. doi: 10.1016/j.cej.2016.07.041.
14. El-Naggar A, Lee SS, Awad YM, Yang X, Ryu C, Rizwan M, et al. Influence of soil properties and feedstocks on biochar potential for carbon mineralization and improvement of infertile soils. Geoderma. 2018;332:100-8. doi: 10.1016/j.geoderma.2018.06.017.
15. Ahmad M, Lee SS, Lee SE, Al-Wabel MI, Tsang DCW, Ok YS. Biochar-induced changes in soil properties affected immobilization/mobilization of metals/metalloids in contaminated soils. J Soils Sediments. 2017;17(3):717-30. doi: 10.1007/s11368-015-1339-4.
16. Xiong Z, Shihong Z, Haiping Y, Tao S, Yingquan C, Hanping C. Influence of NH3/CO2 modification on the characteristic of biochar and the CO2 capture. BioEnergy Res. 2013;6(4):1147-53. doi: 10.1007/s12155-013-9304-9.
17. Qian K, Kumar A, Zhang H, Bellmer D, Huhnke R. Recent advances in utilization of biochar. Renew Sustain Energy Rev. 2015;42:1055-64. doi: 10.1016/j.rser.2014.10.074.
18. Inyang MI, Gao B, Yao Y, Xue Y, Zimmerman A, Mosa A, et al. A review of biochar as a low-cost adsorbent for aqueous heavy metal removal. Crit Rev Environ Sci Technol. 2016;46(4):406-33. doi: 10.1080/10643389.2015.1096880.
19. Parinyakit S, Worathanakul P. Static and dynamic simulation of single and binary component adsorption of CO2 and CH4 on fixed bed using molecular sieve of zeolite 4A. Processes. 2021;9(7):1250. doi: 10.3390/pr9071250.
20. García L, Poveda YA, Khadivi M, Rodríguez G, Görke O, Esche E, et al. Synthesis and granulation of a 5A zeolite-based molecular sieve and adsorption equilibrium of the oxidative coupling of methane gases. J Chem Eng Data. 2017;62(4):1550-7. doi: 10.1021/acs.jced.7b00061.
21. Ko D. Comparison of carbon molecular sieve and zeolite 5A for CO2 sequestration from CH4/CO2 mixture gas using vacuum pressure swing adsorption. Korean J Chem Eng. 2021;38(5):1043-51. doi: 10.1007/s11814-021-0771-y.
22. Zubbri NA, Mohamed AR, Kamiuchi N, Mohammadi M. Enhancement of CO2 adsorption on biochar sorbent modified by metal incorporation. Environ Sci Pollut Res. 2020;27(11):11809-29. doi: 10.1007/s11356-020-07734-3.
23. Esfandian H, Garshasbi V. Investigation of methane adsorption on molecular sieve zeolite (from natural materials). Gas Process J. 2020;8(2):35-50. doi: 10.22108/gpj.2020.121907.1080.
24. Ghalandari V, Hashemipour H, Bagheri H. Experimental and modeling investigation of adsorption equilibrium of CH4, CO2, and N2 on activated carbon and prediction of multi-component adsorption equilibrium. Fluid Phase Equilib. 2020;508:112433. doi: 10.1016/j.fluid.2019.112433.
25. Nazari Kudahi S, Noorpoor AR, Mahmoodi NM. Determination and analysis of CO2 capture kinetics and mechanisms on the novel graphene-based adsorbents. J CO2 Util. 2017;21:17-29. doi: 10.1016/j.jcou.2017.06.010.
26. You S, Ok YS, Tsang DCW, Kwon EE, Wang C-H. Towards practical application of gasification: a critical review from syngas and biochar perspectives. Crit Rev Environ Sci Technol. 2018;48(22-24):1165-213. doi: 10.1080/10643389.2018.1518860.
27. Sevilla M, Fuertes AB. CO2 adsorption by activated templated carbons. J Colloid Interface Sci. 2012;366(1):147-54. doi: 10.1016/j.jcis.2011.09.038.
28. Chiang YC, Juang RS. Surface modifications of carbonaceous materials for carbon dioxide adsorption: a review. J Taiwan Inst Chem Eng. 2017;71:214-34. doi: 10.1016/j.jtice.2016.12.014.
29. Zhang X, Wu J, Yang H, Shao J, Wang X, Chen Y, et al. Preparation of nitrogen-doped microporous modified biochar by high temperature CO2–NH3 treatment for CO2 adsorption: effects of temperature. RSC Adv. 2016;6(100):98157-66. doi: 10.1039/c6ra23748g.
30. Plaza MG, González AS, Pis JJ, Rubiera F, Pevida C. Production of microporous biochars by single-step oxidation: effect of activation conditions on CO2 capture. Appl Energy. 2014;114:551-62. doi: 10.1016/j.apenergy.2013.09.058.
31. Chatterjee R, Sajjadi B, Mattern DL, Chen WY, Zubatiuk T, Leszczynska D, et al. Ultrasound cavitation intensified amine functionalization: a feasible strategy for enhancing CO2 capture capacity of biochar. Fuel. 2018;225:287-98. doi: 10.1016/j.fuel.2018.03.145.